Electronic Supplementary Information (ESI)

PEDOT:PSS and Graphene-Clad Smart Textile Based Wearable Electronic Joule Heater with High Thermal Stability

Abbas Ahmed,[a] Mohammad Abdul Jalil,[b] Md. Milon Hossain,[bc]* Md. Moniruzzaman,[b] Bapan Adak,[d] Samrat Mukhopadhyay,[d] Md. Shohan Parvez,[b] M. Tauhidul Islam[e]

[a]National Institute of Textile Engineering and Research, University of Dhaka, Dhaka 1000, Bangladesh

[b]Department of Textile Engineering, Khulna University of Engineering and Technology, Khulna-9203, Bangladesh

[c]Department of Textile Engineering, Chemistry and Science, North Carolina State University, North Carolina-27606, USA

[d]Department of Textile and Fiber Engineering, Indian Institute of Technology, Delhi 110016, India

[e]Department of Materials Science and Engineering, National Cheng Kung University, Tainan 701, Taiwan (R.O.C.)

*Corresponding author: E-mail: mhossai5@ncsu.edu

Phone: +1 (919) 986 5713

Supplementary Experimental Section: Material Synthesis

Materials S1

Single Jersey, scoured, bleached and knitted 100% cotton fabrics were procured from Texeurop (BD) Ltd, Bangladesh. Fine GO powder of 5 microns size and Sodium dithionite ($Na_2S_2O_4$) were procured from Loba Chemie Pvt. Ltd, India. Conducting polymer, PEDOT:PSS pellets were purchased from Sigma Aldrich (USA). All other chemical reagents such as NaOH (Merck, Germany), polyethylene glycol (PEG-1000, Merck, Germany) were analytical grade and deionized (DI) water was utilized during the experiments.

Experimental S1: Synthesis of rGO

Reduced graphene oxide (rGO) was firstly synthesized from GO by the method reported elsewhere[1]. Briefly, 1mg/mL of GO powder was dispersed into a 120 mL of DI water solution, sonicating for 30 min. Next, the desired amount of reducing agent $Na_2S_2O_4$ was added into the GO dispersion and subsequently, with vigorous stirring, NaOH was added to maintain the pH of the dispersion about 9-10. The mixture was then heated overnight at 90°C in a glycerol bath. After that, the black rGO dispersion was washed multiple times with DI water to remove residual reducing agents and finally, the dispersion was diluted with distilled water to get an rGO concentration of 3.5 mg/mL.

Experimental S2: Preparation of rGO Coated Cotton Textiles

Before rGO treatment, the cotton textile was mercerized with a 5% aqueous solution of NaOH followed by washing and drying. Then the cotton sample was dipped into as-diluted rGO dispersed solution (3.5 mg/mL) and kept for 30 min for sufficient absorption, and subsequently dried in a

vacuum oven at 70°C for 15 min. The same process was repeated four times to obtain a good adherence of rGO on cotton textiles.

Experimental S3: Preparation of rGO/PEDOT:PSS Functionalized Textiles

To further increase the conductivity of rGO treated cotton textiles, the fabrics were functionalized with a conducting polymer (PEDOT:PSS). Firstly, the PEDOT:PSS with a concentration of 30 mg/mL was mixed with 1 vol% PEG-1000 solution, where PEG acts as co-dopant. Then the PEDOT:PSS/PEG solution was probe sonicated for 30 mins and doping was done by keeping the solution overnight with vigorous stirring at room temperature (RT). Later, rGO coated fabrics were dipped into the doped solution and held for 5 mins at ambient temperature and dried in a vacuum oven at 70°C for 15 min. This process was repeated for a maximum of 15 times. Notably, after each dipping cycle, the dopant solution was magnetically stirred for 2 min. By varying the number of dipping cycles, different samples were prepared as described in **Table S1** using different sample codes.

Table S1: Different formulation for the synthesis of CGP heater

Sample Code	Number of dipping cycle in rGO solution	Number of dipping cycle in PEDOT:PSS
CGP1	4	1
CGP2	3	5
CGP3	2	10
CGP4	1	15

Method S1: Testing and Characterizations

The surface and cross-sectional morphology of the uncoated cotton fabric and the fabrics coated with rGO and PEDOT:PSS were analyzed using a SEM (ZEISS Evo 18, special edition). The X-ray Diffraction patterns of pristine cotton textiles and CGPs were recorded with an X-ray diffractometer (Rigaku Ultima IV, Japan). The diffraction pattern of samples was obtained using Cu-Kα radiation (λ = 0.1539 nm) with an operating voltage of 40 kV and an applied current of 40 mA. The 2θ angle ranged from 5° to 30° with a scanning rate of 4°/min. The FTIR spectra of pristine cotton textile and CGPs were measured in the wavelength range 4000-650 cm^{-1} using a Nicolet 6700 FTIR analyzer (Thermo Fisher Scientific, U.S.A.) in ambient condition. An average of 64 scans with a resolution of 4 cm^{-1} was used in attenuated total reflectance (ATR) mode.

The electrical performance of CGPs was measured by a customized gold plated four-probe resistivity meter. The sheet resistance of the composite fabrics was examined at five various positions, and the average sheet resistance was reported**.** The electrothermal characteristics and thermal images of CGPs were determined by an Infrared thermal camera (FLIR E4, Flir) at various applying potentials, and the average value was reported. The washing durability of the CGPs (sample size 3 × 3 cm^2) was tested by washing the samples in a beaker taking 200 ml of water. Each washing cycle was performed for 30 min at 45 °C followed by drying at 80°C for 10 min to simulate the home laundering by hand. The electrical resistance of CGP was repeatedly measured after different washing cycles and the average value was reported.

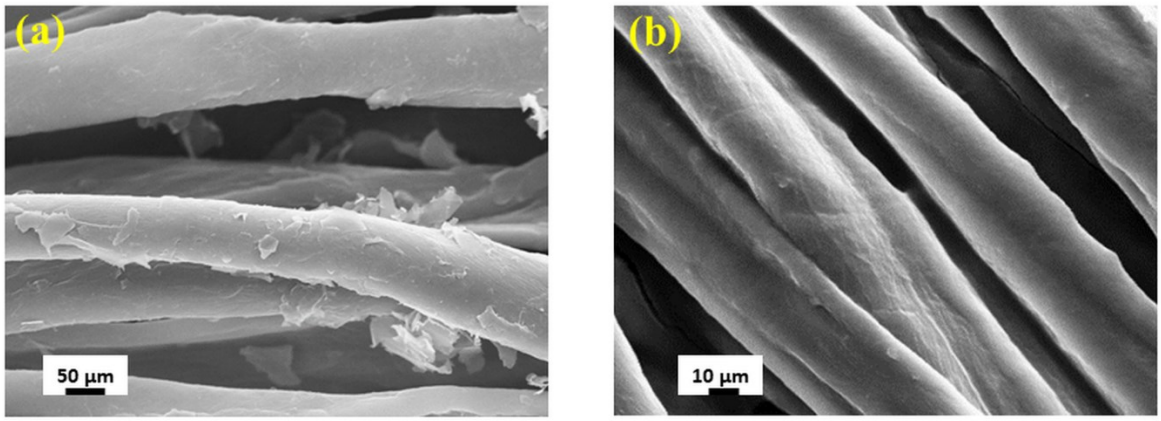

Fig. S1. (a) Cotton fabric treated with rGO and (b) cotton fabric treated with PEDOT:PSS (15 dip cycles)

Method S2

1. Average crystallite size is estimated by Debye-Scherrer formula, $D = \frac{k\lambda}{B\cos\theta}$

Here, D=Average crystallite size (Å), k=Constant=shape factor=0.94, λ = Wavelength for copper =1.54 Å, B (breadth) = Full-width half maximum (FWHM) (Radian), θ_B=Bragg angle=It is the angle of the maximum peak where relative intensity 100%. It varies for the substance to substance (degree).

2. Interplaner distance or d spacing, $d = \frac{\lambda}{2\sin\theta}$
3. Lattice parameters [2]

a=b= $\frac{\lambda}{\sqrt{3}\sin\theta}$

$$c = \frac{\lambda}{\sin\theta}$$

4. Lattic strain for thin film [3]

$$\epsilon = \frac{B}{4\tan\theta}$$

5. Dislocation density and number of crystallites per unit area[4]

Dislocation density $\delta = \frac{1}{D^2}$ (lines/m^2), here D= Average crystallite size

Number of crystallites per unit surface area, **N=** $\frac{t}{D^3}$ **(m^{-2}),** here, t= Thickness, D= Average crystallite size

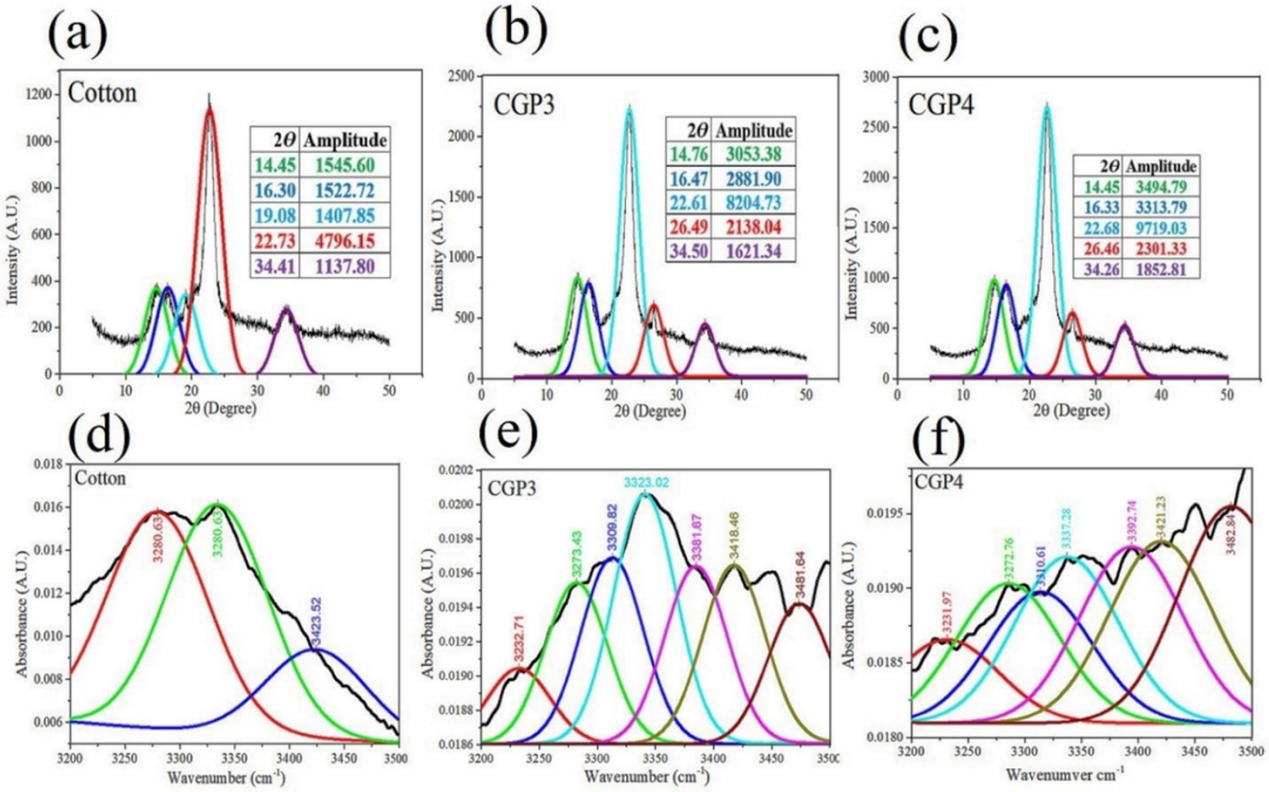

Fig. S2. Gaussian deconvolution curves of XRD peaks of (a) pristine cotton; (b) CGP3 (2 cycles of rGO and 10 cycles of PEDOT:PSS dipping); (c) CGP4 (rGO and 15 cycles dipping of PEDOT:PSS) and FTIR peak of (d) pristine cotton; (e) CGP3 ; (f) CGP4

The characteristic crystalline (200) and amorphous ($10\bar{1}$) plane of cotton were considered for crystallinity index determination following the so-called Segal method which is termed as "S-CI" throughout the manuscript. But it is considered that the crystallinity index is proportional to the peak area rather than the peak height[5]. So, the peak deconvolution of crystalline and amorphous regions was utilized for CI determination according to so called Harmans methods which is termed as "H-CI" throughout the manuscript[5].

For cotton, CGP3 and CGP4 the S-CI values were determined as 70.34, 62.05 and 65.09%, respectively, whereas the H-CI values were 31.47, 46.39 and 48.23%, respectively. Although the trend of S-CI and H-CI values of the CGPs were similar, but pristine cotton exhibited as opposite. So, total crystallinity index (TCI), empirical crystallinity index which is most popularly known as lateral oxygen index (LOI), and crystallinity index were calculated from the FTIR spectrums [5].

Method S3

1. TCI= $\frac{Absorbance\ intensity\ at\ 1360.96\ cm-1}{Absorbance\ intensity\ at\ \ 2898.3\ cm-1}$
2. LOI= $\frac{Absorbance\ intensity\ at\ 895.8\ cm-1}{Absorbance\ intensity\ at\ \ 1472\ cm-1}$
3. IR-CI= $\frac{Absorbance\ intensity\ at\ 1360.69\ cm-1}{Absorbance\ intensity\ at\ 662.8\ cm-1}$
4. HBI= $\frac{Absorbance\ intensity\ at\ \ 3334.26\ cm-1}{Absorbance\ intensity\ at\ 1313.7\ cm-1}$

5. AF= $\frac{FWHM\ at\ 3654cm-1}{FWHM\ at\ 3560cm-1}$

The energy of the hydrogen bond (E_H) and the hydrogen bond distance *R* values were calculated by using the following equations[6]-

6. $E_{H=}\frac{1}{k}.[\frac{\nu_0-\nu}{\nu}]$, here, ν_0 is the standard frequency of free -OH group (3650 cm^{-1}), ν is the frequency of the bonded –OH (cm^{-1}) groups and k is a constant $\frac{1}{k}$ = (2.625 × 10^2 kJ).
7. R = 2.84 - $\frac{\Delta\nu\ (c/m)}{4430}$, here ν is the stretching frequency of the measured samples.

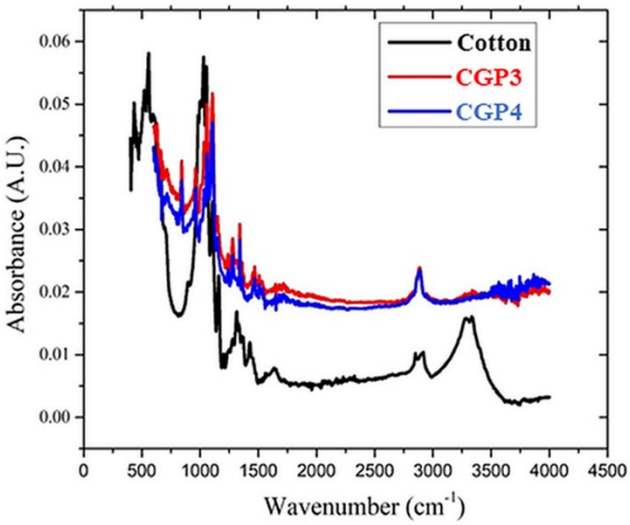

Fig. S3. FTIR absorbance spectra of cotton and different CGP samples

Table S2. Effect of rGO and PEDOT:PSS embedding on inter and intra-molecular hydrogen bonding energy and distances of cotton cellulose and their corresponding sheet resistance (Rs.).

Sample	Peak wavenumber and absorbance intensities (Abs.) of Cellulose-I (Cell.-I) and Cellulose-II (Cell.-II) allomorph				Bond types	E_H (kJ)	R (Å)	Rs. (Ω/sq)
	Cell.-I (cm^{-1})	Abs. (A.U.)	Cell.-II (cm^{-1})	Abs. (A.U.)				
Cotton	3280.63	0.0158			Inter O(6)H---O(3)	26.753	2.7673	10^8 -10^9
	3334.08	0.0161			Intra O(3)H---O(5)	22.726	2.7799	
	3423.52	0.0094			Intra O(2)H---O(6)	16.253	2.8002	
CGP3	3232.71	0.0186			Inter O(6)H---O(3)	30.062	2.7569	263
	3273.43	0.0197			Inter O(6)H---O(3)	27.185	2.7659	
			3309.82	0.01979	OH Inter H-bond	24.524	2.7743	
			3323.02	0.01984	OH Intra H-bond	23.445	2.7777	
	3337.81	0.0202			Intra O(3)H---O(5)	22.366	2.7810	
			3381.67	0.01968	OH Intra H-bond	19.346	2.7906	

	3418.46	0.0199			Intra O(2)H---O(6)	16.685	2.7989	
			3481.64	0.02	OH Intra H-bond	12.226	2.8129	
CGP4	3231.97	0.019			Inter O(6)H---O(3)	30.062	2.7569	153
	3272.76	0.0191			Inter O(6)H---O(3)	27.185	2.7659	
			3310.61	0.0192	OH Inter H-bond	24.524	2.7743	
			3325.94	0.01914	OH Intra H-bond	23.445	2.7777	
	3337.28	0.0194			Intra O(3)H---O(5)	22.510	2.7806	
			3382.74	0.01923	OH Intra H-bond	19.346	2.7906	
	3421.23	0.0197			Intra O(2)H---O(6)	16.469	2.7996	
			3482.84	0.01971	OH Intra H-bond	12.082	2.8134	

The main contrast between cellulose Iα and cellulose 1β tends to the dislocation of cellulose sheets. The allomorph I has dislocation of +C/4, where allomorph II has a relative disorder which alter between +C/4 and -C/4, which afterward make a different in relative occupancy of the structure. In cellulose Iα, 55% of H-atoms are engaged in hydrogen bond formation, whereas 1β is tightly packed having a relative occupancy 70-80%[7]. The shifting of FTIR peaks over 3200-3600 cm^{-1} implies that , CGP3 and CGP4 have an antiparallel arrangement of the cellulose chains that are oriented in a 3D H-bonded channel, whereas the pristine cotton (cellulose I) has a 2D shaped H-bonded layers on top of each other of cellulose I.

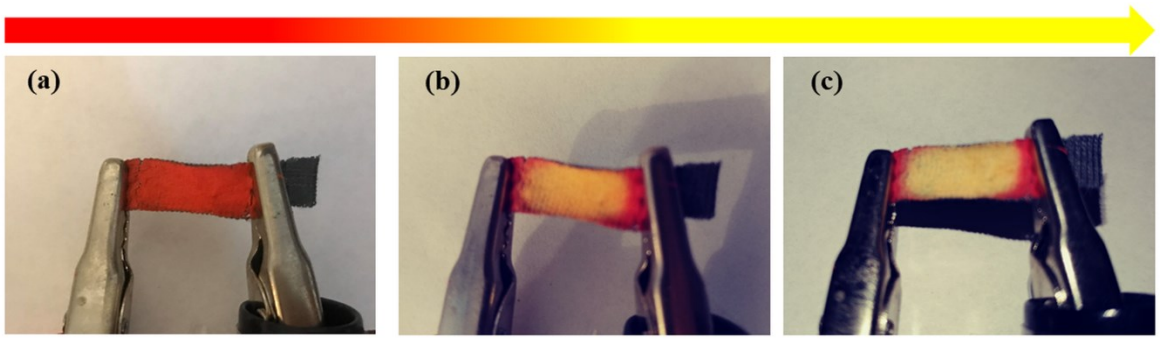

Fig. S4. (a-c) Digital camera images of electrochromic transition of CGN heater at different voltages.

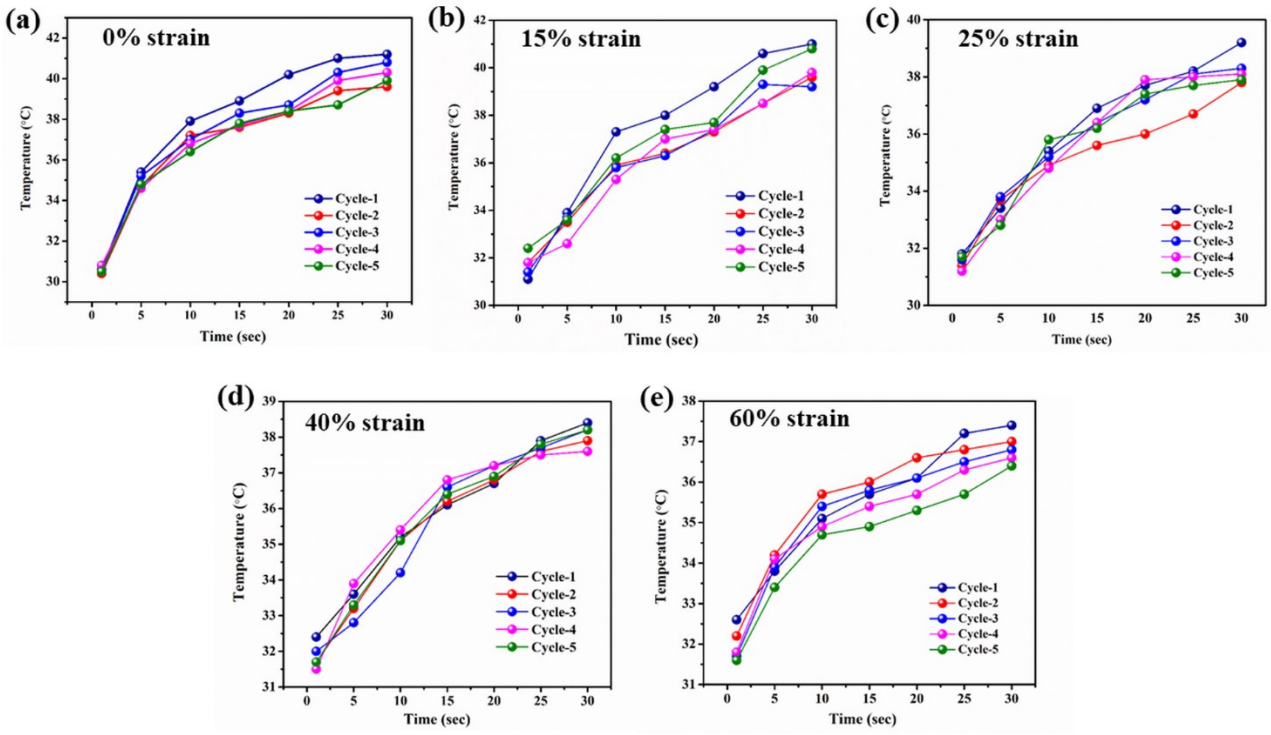

Fig. S5. Electrothermal performance of the CGP heater under stretching cycles of (a) 0% strain; (b) 15% strain; (c) 25% strain; (d) 40% strain and (e) 60% strain.

Table S3. Comparison table of electrical heating performance of our fabricated CGP Joule heater with most recent others.

Heater	Electrical properties	Maximum temperature [^{o}C] @ applied voltage [V]	Temperature variation (%) @ applied strain	ref
Cotton/rGO/PEDOT:PSS (CGP)	150 Ω/sq.	70 @ 30	~9.0% @ 60%	Present work
Carbonized modal textile (CMT)	1.89 Ω/sq.	100 @ 3.5	16.7% @ 70%	[8]
PU/CB/Fabric	71 < Ω/cm	50 @ 20	N/A	[9]
CB/CF	~ (25-28) kΩ/sq.	54 @ 5	N/A	[10]
MWCT/Graphene/Cotton	33.2 Ω/sq. for MWCNT and 29.8 Ω/sq. for Graphene	53.2 @ 27 for MWCNT and 66.2 @ 27 for Graphene	N/A	[11]

MXene/PPy/PET	2.33 Ω/sq.	79 @ 4	N/A	[12]
Graphene/Tourmaline/WPU/Cotton	N/A	56.2 @ 8	N/A	[13]
Ag NFs/Fabric/Pt NF	25 Ω/sq.	41.3 @ 3	N/A	[14]
rGO/PET	48 Ω/sq.	73 @ 10	N/A	[15]
Silver yarn/GNP/PVDF-HFP	4.4 × 101 ± 1.3 × 101 Ω/sq.	48 @ 5	N/A	[16]

Table S4. Wash durability performance comparison of fabricated CGP Joule heater with others

Textile Substrate	Active Materials	Fabrication Method	#Wash Cycles	Increase in Resistance	Application	Ref
Cotton fabric	rGO/PEDOT:PSS	Coating	15	153.28 to 155.41 Ω/sq.	Wearable Joule heater	Present work
Cotton fabric	rGO	Coating	10	36.94 to 139.09 kΩ/sq.	Strain sensor	[1]
Non-woven fabric	rGO/CNT	Nano-soldering	6	30.25 to 36.94 kΩ	strain sensor	[17]
Silk	rGO	Coating	10	~5 to 6.5 kΩ/cm	UV blocking	[18]
Nylon/PU fabric	rGO	Coating	8	112 to 158 kΩ/m^2	strain sensor	[19]
Kevlar threads	PEDOT:PSS	Coating	4	15 to 40 Ω	E-textiles	[20]

Cotton fabric	Graphene nanoplate/PU	Pad-dry-cure	10	2.94×10^{-1} to 3.35×10^{-1} Ωm	UV blocking	[21]
Cotton fabric	Ag/Cu	electroless deposition	10	0.13-0.135 kΩ/sq.	Anti-bacterial textiles	[22]
Cotton roving	CNT	N/A	10	A very small increase in resistance	Electro-thermochromic textiles	[23]
Polyester	PEDOT:PSS	Spray-coating	5	12.10 to 50 Ω/sq.	Wearable heater	[24]

References

1 N. Karim, S. Afroj, S. Tan, P. He, A. Fernando, C. Carr and K. S. Novoselov, *ACS Nano*, 2017, **11**, 12266–12275.

2 K. L. Foo, U. Hashim, K. Muhammad and C. H. Voon, *Nanoscale Res. Lett.*, 2014, **9**, 429.

3 D. Fang, C. Li, N. Wang, P. Li and P. Yao, *Cryst. Res. Technol.*, 2013, **48**, 265–272.

4 A. Moses Ezhil Raj, S. Mary Delphine, C. Sanjeeviraja and M. Jayachandran, *Phys. B Condens. Matter*, 2010, **405**, 2485–2491.

5 S. Rongpipi, D. Ye, E. D. Gomez and E. W. Gomez, *Front. Plant Sci.*, 2019, 9, 1894.

6 T. Tribulová, F. Kačík, D. V. Evtuguin, I. Čabalová and J. Ďurkovič, *Cellulose*, 2019, **26**, 2625–2638.

7 A. Santmartí and K.-Y. Lee, in *Nanocellulose and Sustainability*, CRC Press, 2018, pp. 67–86.

8 M. Zhang, C. Wang, X. Liang, Z. Yin, K. Xia, H. Wang, M. Jian and Y. Zhang, *Adv. Electron. Mater.*, 2017, **3**, 1700193.

9 L. R. Pahalagedara, I. W. Siriwardane, N. D. Tissera, R. N. Wijesena and K. M. N. De Silva, *RSC Adv.*, 2017, **7**, 19174–19180.

10 R. Islam, N. Khair, D. M. Ahmed and H. Shahariar, *Mater. Today Commun.*, 2019, **19**, 32–38.

11 J. Cui and S. Zhou, *J. Mater. Chem. C*, 2018, **6**, 12273–12282.

12 Q. W. Wang, H. Bin Zhang, J. Liu, S. Zhao, X. Xie, L. Liu, R. Yang, N. Koratkar and Z. Z. Yu, *Adv. Funct. Mater.*, , DOI:10.1002/adfm.201806819.

13 Y. Hao, M. Tian, H. Zhao, L. Qu, S. Zhu, X. Zhang, S. Chen, K. Wang and J. Ran, *Ind. Eng. Chem. Res.*, 2018, **57**, 13437–13448.

14 J. Huang, Y. Li, Z. Xu, W. Li, B. Xu, H. Meng, X. Liu and W. Guo, *Nanotechnology*, 2019, **30**, 325203.

15 D. Wang, D. Li, M. Zhao, Y. Xu and Q. Wei, *Appl. Surf. Sci.*, 2018, **454**, 218–226.

16 H. Kim and S. Lee, *Polymers (Basel).*, 2019, **11**, 928.

17 Z. Tang, D. Yao, D. Du and J. Ouyang, *J. Mater. Chem. C*, 2020, **8**, 2741–2748.

18 J. Cao and C. Wang, *Appl. Surf. Sci.*, 2017, **405**, 380–388.

19 G. Cai, M. Yang, Z. Xu, J. Liu, B. Tang and X. Wang, *Chem. Eng. J.*, 2017, **325**, 396–403.

20 C. M. Choi, S. N. Kwon and S. I. Na, *J. Ind. Eng. Chem.*, 2017, **50**, 155–161.

21 X. Hu, M. Tian, L. Qu, S. Zhu and G. Han, *Carbon N. Y.*, 2015, **95**, 625–633.

22 T. Suryaprabha and M. G. Sethuraman, *J. Alloys Compd.*, 2017, **724**, 240–248.

23 M. Yang, J. Pan, L. Luo, A. Xu, J. Huang, Z. Xia, D. Cheng, G. Cai and X. Wang, *Smart Mater. Struct.*, , DOI:10.1088/1361-665X/ab21ef.

24 F. Gong, C. Meng, J. He and X. Dong, *Prog. Org. Coatings*, 2018, **121**, 89–96.